Role of peptide-peptide interactions in stabilizing peptide-wrapped single-walled carbon nanotubes: A molecular dynamics study

3 AUTHORS:

Chi-Cheng Chiu
Argonne National Laboratory
34 PUBLICATIONS **424** CITATIONS

SEE PROFILE

Gregg R Dieckmann
University of Texas at Dallas
35 PUBLICATIONS **2,141** CITATIONS

SEE PROFILE

Steven O Nielsen
University of Texas at Dallas
52 PUBLICATIONS **906** CITATIONS

SEE PROFILE

Role of Peptide–Peptide Interactions in Stabilizing Peptide-Wrapped Single-Walled Carbon Nanotubes: A Molecular Dynamics Study

Chi-cheng Chiu, Gregg R. Dieckmann, Steven O. Nielsen

Department of Chemistry and Alan G. MacDiarmid NanoTech Institute,
The University of Texas at Dallas, 800 West Campbell Road, Richardson, TX 75080

ABSTRACT:

Single-walled carbon nanotubes (SWNTs) have unique properties and are projected to have a major impact in nanoscale electronics, materials science, and nanomedicine. Yet, these potential applications are hindered by the need for sample purification to separate SWNTs from each other and from metallic catalyst and amorphous carbon present in as-synthesized samples. Common purification strategies involve dispersing SWNTs as individual tubes in aqueous solution. Towards this end, a designed helical peptide was shown to be excellent at dispersing SWNTs. However, the molecular details of the peptide-SWNT and peptide-peptide interactions await elucidation. Here we explore these molecular interactions using fully atomistic molecular dynamics simulations of peptide-wrapped SWNTs. We characterize the interactions by measuring the aromatic residue-to-SWNT surface distance, the peptide amphiphilicity, the peptide-SWNT crossing angle, the peptide-SWNT contact area, the peptide helix axis-to-axis distance, and the inter-peptide hydrogen bonding. We find that the peptides collectively tilt with respect to the SWNT long axis, are α-helical, and form interpeptide hydrogen bonds through their lysine and glutamate residues, which helps to stabilize the multipeptide/SWNT complex. All hydrophobic residues interact with the SWNT and are sequestered from water. The picture that emerges from this study gives insight into subsequent peptide design. © 2009 Wiley Periodicals, Inc. Biopolymers (Pept Sci) 92: 156–163, 2009.

Keywords: molecular dynamics; peptide design; carbon nanotube

INTRODUCTION

Single-walled carbon nanotubes (SWNTs) are hollow cylinders formed by seamlessly wrapping a single graphene sheet. They are characterized by a pair of integers (n,m) called the chiral vector which is the graphene sheet translation vector defining the axial direction of the nanotube; the nanotube diameter d is given by the formula $d = [3(n^2 + nm + m^2)]^{1/2}(d_{cc}/\pi)$ where d_{cc} is the carbon–carbon bond length.[1] Because of their extraordinary electrical and mechanical properties, SWNTs are thought to have many potential applications in biological systems, electronic devices, and energy conservation devices.[2] Unfortunately, carbon nanotubes are extremely hydrophobic which leads to uncontrolled SWNT aggregation. This makes it difficult to purify and separate SWNTs, and hence difficult to assemble them into useful structures. Thus, extensive studies have been focused on dispersing SWNTs in aqueous solution and increasing their water solubility, with the end goal of preparing controlled dispersions for subsequent manipulation.

Different methods exist towards this goal, which can broadly be classified into techniques which either covalently or noncovalently modify the SWNT surface.[3,4] Covalent modifications provide functionalized SWNTs in which various functional groups are attached to the SWNTs through, for example, esterification, amidation, or carboxylation. Sun et al. showed the potential biological application of SWNTs by chemically attaching proteins to nanotubes via amidation and generating what they called "immuno carbon nanotubes."[5–7] One major disadvantage of covalent modification is that the electronic properties of the SWNTs can be strongly disrupted by a high degree of functionalization.

In contrast, the noncovalent modification of SWNTs, which can be achieved by using surfactants or polymers, conserves the intrinsic sp^2 hybridization and conjugation of the nanotube atoms and prevents any disruption to the SWNT electronic structure. These molecules interact with SWNTs through nonbonding interactions and are not chemically attached to the nanotube. Unlike the covalently bound case, the resulting complexes are generally unstable to external perturbations such as dilution.[8–12] One of the most important nonbonding interactions is the aromatic π-π (π-stacking) interaction. Chen et al. functionalized SWNTs by using amphiphilic molecules with pyrene at one end to interact with the SWNT side wall through the π-stacking interaction.[13] Deoxyribonucleic acid (DNA) has also been studied both experimentally and computationally for its ability to disperse and separate SWNTs through the π-stacking interaction between SWNTs and DNA bases.[14–16] Other studies on buckyball-specific antibodies also revealed the importance of having aromatic residues, such as tryptophan, phenylalanine, and tyrosine, at the proposed C_{60} binding site.[17–19]

To prepare SWNTs for possible biological applications and to have good noncovalent functionalization, Dieckmann et al. designed a 29-residue peptide, named nano-1, which can fold into an amphiphilic α-helical conformation, interact with the aromatic surface of SWNTs, and disperse them in aqueous solution.[20–23] The nano-1 peptide has four heptad-residue repeats, denoted $(a,b,c,d,e,f,g)_4$, with valine (Val) at the a position and phenylalanine (Phe) at the d position. The a and d positions form the hydrophobic face of the α-helix, whereas the b,c,e,f,g positions are occupied by hydrophilic residues.[20,24] From circular dichroism (CD) data, nano-1 shows high α-helical content in aqueous solution in the presence of SWNTs.[20] Raman spectroscopic studies showed major shifts in the peaks corresponding to the radial breathing modes of the nanotubes, suggesting the SWNTs are wrapped by the peptide in aqueous solution. Atomic force microscopy (AFM) experiments showed that nano-1 disperses SWNTs with a diameter range from 0.7 nm to

3.3 nm.[23] Transmission electron microscopy (TEM) images showed that the peptide helix/SWNT crossing angle ranges from 10° to 20°.[21] By altering the number of heptad-residue repeats and the number of Phe residues, it was found that peptides with fewer Phe residues had a decreased ability to disperse SWNTs, suggesting that nano-1 mainly uses Phe residues to interact with the SWNT side wall through the π-stacking effect.[22] However, due to instrumental limitations, the peptide/SWNT samples for the microscopy studies were dehydrated before imaging.[20–23] It is not clear if the resulting picture of molecular interactions gives insight into the aqueous solution structure. Thus, in this study, we use computer simulations to study the interaction between the nano-1 peptide and SWNTs in aqueous solution.

The α-helical conformation of nano-1 is amphiphilic and hence should be disfavored for an isolated peptide in aqueous solution. Experimental data has shown that, in aqueous solution, nano-1 self-associates into three helix bundles (Ortiz, A., Ph.D. Thesis, The Univeristy of Texas at Dallas, 2008). Thus, in the presence of SWNTs, the peptide self-association is in competition with the peptide/SWNT association. One could ask whether the peptide acquires an α-helical conformation before or after the peptide adsorbs on the SWNT surface. A similar question was addressed by Nymeyer et al. using replica exchange molecular dynamics (MD) techniques for the case of a short helical peptide inserting into a lipid bilayer.[25] Unfortunately, such a study requires formidable computational resources; we have therefore chosen to focus our attention on the structural and dynamical properties of the preformed peptide/SWNT complex. In a previous study, we used fully atomistic molecular dynamics simulations to investigate a single nano-1 peptide at three different water/hydrophobic interfaces: water/oil, water/graphite, and water/SWNT.[26] It was demonstrated that the α-helical peptide uses its amphiphilic character optimally at the water/SWNT interface. However, nano-1 was designed not only to form an amphiphilic α-helix at the water/SWNT interface, but also to participate in hydrogen bonding (H-bonding) with adjacent peptides through glutamate (Glu) and lysine (Lys) residues.[20,27] In this study, we extend our previous work to focus on peptide–peptide interactions and their role in stabilizing nano-1 - SWNT dispersions.

It has been suggested from molecular mechanics modeling that an (8,8) SWNT is stabilized by a bundle of six nano-1 peptides.[20] In this study, we performed MD simulations of a six peptide bundle around an (8,8) SWNT (hereafter referred to as a hexamer/(8,8) SWNT complex) and, separately, a five peptide bundle around a (6,6) SWNT (hereafter referred to as a pentamer/(6,6) SWNT complex) to examine the peptide–peptide interactions and their effect on the peptide-nanotube conformation.
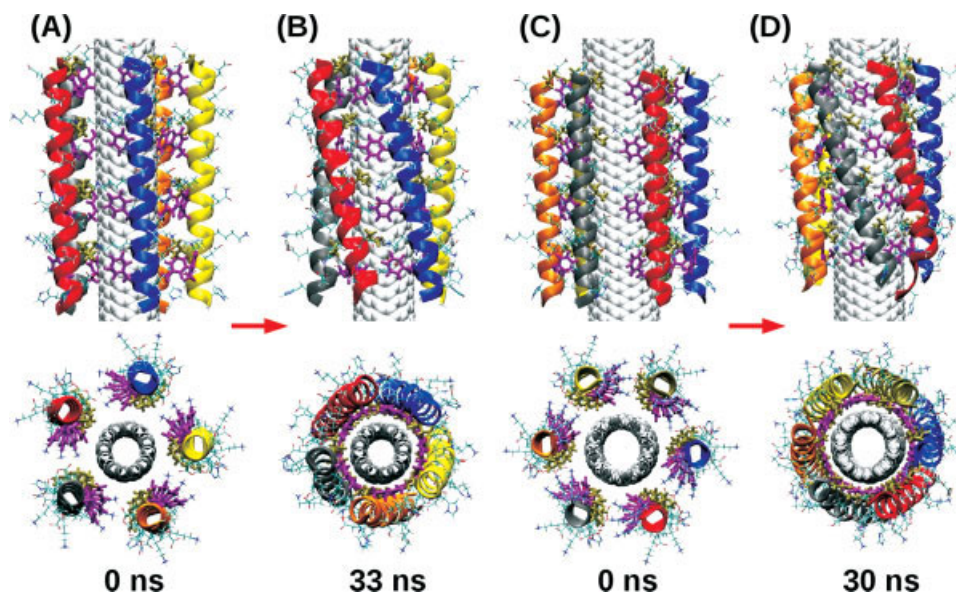
FIGURE 1 Snapshots from MD simulations for pentamer/(6,6) SWNT (A and B) and hexamer/(8,8) SWNT (C and D) systems. A and C illustrate the initial conformations, whereas B and D illustrate the final conformations after 33 ns of simulation for pentamer/(6,6) SWNT and 30 ns of simulation for the hexamer/(8,8) SWNT system, respectively. The upper panels display views perpendicular to the SWNT long axis, and the lower panels display perspectives along the SWNT long axis. SWNTs are represented using the vdW model, and peptide backbones are visualized using ribbons. Side chains are shown with a stick model, where Phe and Val residues are emphasized using thicker lines colored in purple and tan, respectively. Water molecules have been removed for clarity. The images are created using the VMD package.[37] The peptides are marked as P0 (blue), P1 (red), P2 (gray), P3 (orange), and P4 (yellow) for both systems, and in addition P5 (tan) for the hexamer/(8,8) SWNT system. The P1 peptide in (D) has slightly unfolded at its C-terminus and uses its His residue to interact with the SWNT sidewall.

METHODS

All the molecular dynamics simulations in this study were carried out using the program NAMD version 2.6b[28] with the CHARMM31 force field.[17,29–31] All of the simulations were performed with the isothermal-isobaric (NPT) ensemble at 300 K and 1 atm. Periodic boundary conditions were used in all three dimensions. The pressure was controlled using the Nosé-Hoover Langevin piston method, and the temperature was maintained by Langevin dynamics. A time step of 2 fs was used to integrate the equations of motion. The nonbonded interactions were calculated every time step, and full electrostatic interactions were calculated every two time steps. The SHAKE/RATTLE algorithm was used to constrain the bonds between hydrogen atoms and heavy atoms at their equilibrium values.[32,33] The water model used for all systems is the TIP3P model.[34] System coordinates were saved every 10 ps during each simulation for subsequent data analysis.

For MD simulations, the starting peptide coordinates of the amino acid sequence E(VEAFEKK)(VAAFESK)(VQAFEKK)(VEAFEHG) were generated in a perfect α-helical conformation with the backbone dihedral angles $\Phi = -65°$ and $\Psi = -40°$, as reported in our previous study.[26] The nanotubes used in this study were (6,6) and (8,8) SWNTs with 80 cell replications. The nanotube setup followed our previous study[26]: the long axis of the nanotube was immobilized on the x-axis by adding an additional elastic force, with a 1 kcal/mol/Å[2] force constant and the

nanotube radius as the equilibrium distance, to the nanotube carbon atoms to prevent the nanotube from bending or tilting away from the x-axis. The periodic boundary conditions create an effectively infinitely long nanotube to avoid end effects and to focus attention on studying the peptide interactions with non-defective SWNT side walls.

Previous molecular mechanics modeling suggested a stable nano-1 peptide/SWNT complex where an (8,8) SWNT with a radius of 5.4 Å was surrounded by six nano-1 peptides.[20] Here, a similar system was studied using MD simulation: an (8,8) SWNT was ensheathed by six nano-1 peptides labeled as P0, P1, P2, P3, P4, and P5. Each peptide center of mass was equally spaced and placed 9 Å away from the SWNT surface. We chose to study a single multipeptide layer with zero vertical offset (along the SWNT long axis) between the peptides. Other alignments (offsets) are possible, and in reality likely, but their study would require using two or more layers so that the offsets interdigitate; this would involve a prohibitively large system size (more than double the ∼210,000 atoms constituting the hexamer/(8,8) SWNT system). The choice of offset would not be expected to affect the peptide-peptide interactions, hence the results we report for the single layer system should be representative of the general case. The resulting system was then solvated in a 198.8 Å × 108.5 Å × 106.0 Å box with 67,470 water molecules as displayed in Figure 1C. A 30-ns simulation was conducted on this system.

A pentamer/(6,6) SWNT system was also studied for comparison to the above hexamer/(8,8) SWNT system and with our earlier study on a single nano-1/(6,6) SWNT complex.[26] Five peptides were judged to optimally wrap a (6,6) SWNT because the aromatic ring center of the Phe sidechains have been shown to be ~3.5 Å away from the nanotube surface.[26] We can assume that the six peptides surround the (8,8) nanotube at a distance of about 8.9 Å (3.5 Å + 5.4 Å, the radius of the (8,8) SWNT) which gives a circumference of 55.9 Å; thus, each nano-1 peptide occupies approximately an arc length of 9.3 Å. Applying these values to the (6,6) SWNT with a 4.1 Å radius, we estimated that five peptides could wrap a (6,6) SWNT. Thus, in this study five peptides, labeled as P0, P1, P2, P3, and P4, were equally spaced around a (6,6) SWNT in an analogous manner to the hexamer system. The system was then solvated by 64,371 water molecules in a 198.8 Å × 104.5 Å × 105.5 Å box as displayed in Figure 1A. The system was simulated for 33 ns. Both the pentamer and hexamer systems were considered to have reached equilibrium when the peptide α-helicities and the root-mean-square deviations of the peptide backbones with respect to the initial conformations were converged.

To characterize the conformational changes of the peptide, the α-helical content of the peptide was calculated based on the Lifson-Roig model,[35] where residue i is marked α-helical only if its dihedral angle pair (Φ_i, Ψ_i) and those of the two adjacent residues $[(\Phi_{i-1}, \Psi_{i-1})$ and $(\Phi_{i+1}, \Psi_{i+1})]$ lie in the region $\Phi = -65 \pm 35°$ and $\Psi = -37 \pm 30°$. Thus, for the 29 residue nano-1 peptide with N-terminal acetylation and C-terminal amidation, the maximum number of residues that can be marked α-helical is 27. The α-helicity of the peptide was calculated by counting the number of α-helical residues and dividing by 27, resulting in a value between zero and one.

The crossing angle is defined as the angle between the α-helix axis and the nanotube long axis. The α-helix axis is defined based on Kahn's method in which a partial axis is defined by four residues.[36] Hence, 26 partial axes can be found for nano-1. The axis of the entire helix is calculated through a linear least squares method accounting for all partial axes.

The distances between each pair of peptides were studied to characterize the peptide–peptide interactions. The peptide–peptide distance was defined as the distance between the two helix axes in the plane perpendicular to the SWNT long axis passing through the center of mass of all the peptides.

The contact area between the protein and the SWNT was calculated as:

$$A_{contact} = \frac{1}{2}(A_{protein} + A_{NT} - A_{all})$$

where $A_{protein}$ is the molecular surface area for the entire protein, A_{NT} is the corresponding quantity for the nanotube, and A_{all} is the surface area of the protein-nanotube complex. The molecular surface areas were calculated using the program MSMS.[37] The ratio of $A_{contact}$ to $A_{protein}$ was calculated to describe the degree of contact.

The distances between the centers of the aromatic rings of the Phe sidechains and the surface of the nanotube were analyzed to characterize the π-π stacking orientation of the Phe residues with respect to the nanotube sidewall. The Phe-to-SWNT distance $d_{Phe-SWNT}$ was calculated by subtracting the SWNT radius from the "Phe ring center to SWNT long axis" distance.[26]

The number of H-bonds formed between adjacent peptides were counted to characterize the peptide-peptide interaction inside the multi- nano-1/SWNT complexes. We defined an H-bond by the following criterion: given a heteroatom A attached to an H-atom and another heteroatom B not bonded to A, an H-bond is formed only if the distance between two heavy atoms is smaller than 4 Å and the A-H-B angle is smaller than 30°.[38]

RESULTS AND DISCUSSION

Peptide Conformation in the Multipeptide/SWNT Complexes

The pentamer/(6,6) SWNT and hexamer/(8,8) SWNT complexes were set up to be as comparable as possible by using the same arc length of contact with the nanotube for each peptide (see Methods). However, the difference in diameter between the two SWNTs results in a different packing tightness between the two peptide-wrapped systems. This difference clearly manifests itself in the data presented below.

After 30 ns of MD simulation, both the pentamer/(6,6) SWNT complex and the hexamer/(8,8) SWNT complex have reached equilibrium; representative snapshots of the pentamer system are shown in Figures 1A and 1B, and of the hexamer system in Figures 1C and 1D. H-bonds are formed between adjacent peptides which help to stabilize the multipeptide/SWNT complexes. All peptides remain α-helical and form interpeptide H-bonds through their Lys and Glu residues; all hydrophobic residues interact with the SWNT and are sequestered from water. The peptides in both complexes collectively tilt from an initially parallel alignment with the SWNT long axis (see Figure 1). In the hexamer/(8,8) SWNT complex, the P1 peptide has slightly unfolded at its C-terminus due to terminal fraying and uses residue His28 to interact with the SWNT sidewall suggesting a favorable interaction between the imidazole side chain and the SWNT side wall.

The α-helicity analysis is shown in Figure 2. For the pentamer/(6,6) SWNT complex, the helicities of all five peptides are ≥90% which is similar to the single peptide/(6,6) SWNT system of our previous study.[26] For the hexamer/(8,8) SWNT complex, the P1 peptide slightly unfolds at its C-terminus from 5 to 20 ns of the simulation, but then subsequently refolds. The interaction between the P1 His28 residue with the SWNT sidewall decreases the overall α-helicity of the P1 peptide to ~85%. The P1 peptide partial unfolding slightly modifies the packing of the hexamer which stabilizes the structure of the other peptides (they now have less room than before P1 unfolded). In the pentamer/(6,6) SWNT complex, the variation of the peptide α-helicities with time is smaller than in the hexamer/(8,8) SWNT complex.

The crossing angle of the peptides in the pentamer/(6,6) SWNT system ranges from 11° to 16° after the first 10 ns of
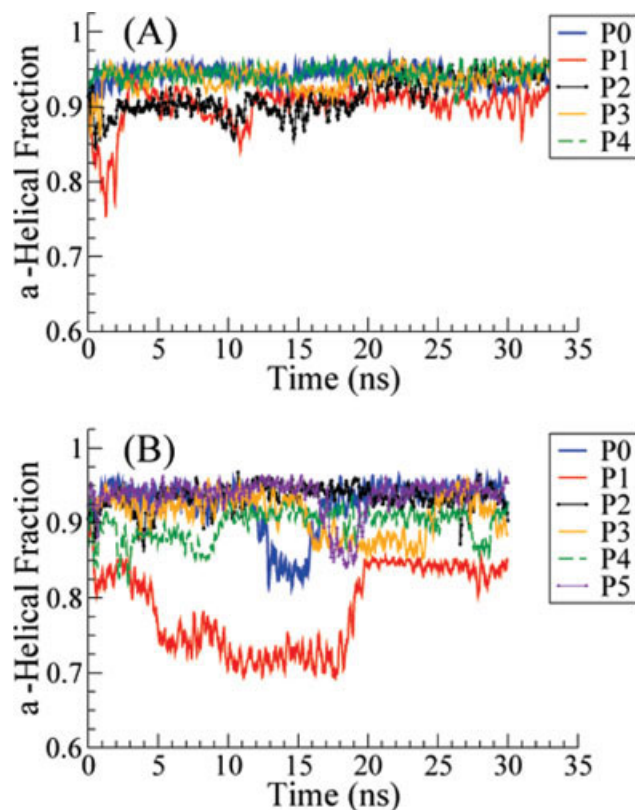
FIGURE 2 The α-helicity for each nano-1 peptide in (A) pentamer/(6,6) SWNT and (B) hexamer/(8,8) SWNT systems as a function of time. The peptides retain a high α-helical content in both systems. In the hexamer/(8,8) SWNT system, the α-helicity decrease of P1 during 5 to 20 ns is due to the C-terminal fraying and interaction with the SWNT using the His residue. The peptides are marked as P0 (blue), P1 (red), P2 (black), P3 (orange), and P4 (green dash) for both systems, and in addition P5 (purple) for the hexamer/(8,8) SWNT system.

the simulation as shown in Figure 3A. All five peptides have similar crossing angle values, with a mean of ∼13°. This indicates that all peptides adopted similar conformations and formed a symmetrical pentamer/(6,6) SWNT complex. Figure 3B illustrates the crossing angles for the hexamer/(8,8) SWNT complex. The angle for each peptide is around 13° after 10 ns simulation, but has a larger variation than in the pentamer/(6,6) SWNT system. From both the α-helicity and crossing angle analyses, larger fluctuations are observed in the hexamer/(8,8) SWNT system than in the pentamer/(6,6) SWNT system. This implies that the peptides in the hexamer/(8,8) SWNT complex are not as tightly packed as in the pentamer/(6,6) SWNT complex.

Figure 4 illustrates the comparison of the average crossing angles of both multipeptide/SWNT systems and the crossing angle of a single nano-1 peptide/(6,6) SWNT complex.[26] The crossing angle in the single peptide system has a much wider

angle distribution from 5° to 25° than the narrow angle distribution of 11° to 17° for both the pentamer/(6,6) SWNT and hexamer/(8,8) SWNT complexes. For both multipeptide systems, the most probable angle is 13°, which is different from the most probable angle of 17° for the single peptide system.[26] For all three systems, the most probable angles are consistent with the crossing angle range of 10° to 20° from experimental data.[21] The peptide–peptide interactions limit the peptide's motion on the SWNT, which suppresses the crossing angle thermal fluctuations. The shift in the most probable crossing angle suggests that the interpeptide interactions are significant. Nonetheless, the overall angle distributions of the multipeptide systems fall inside the distribution range of the single peptide system, suggesting that the interpeptide interactions do not destabilize the peptide-SWNT interactions.

Peptide–Peptide Interactions in the Multipeptide/SWNT Complexes

Figure 5 illustrates the axis-to-axis distances of each pair of adjacent α-helical peptides in the multipeptide/SWNT com-
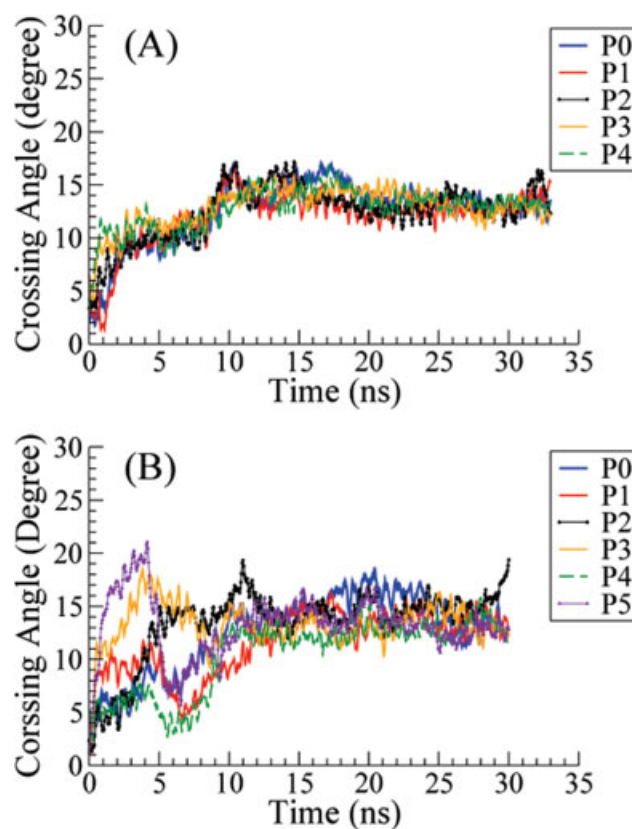

FIGURE 3 The crossing angle formed between the peptide helical axis and the SWNT long axis in the (A) pentamer/(6,6) SWNT and (B) hexamer/(8,8) SWNT systems as a function of time. The peptides are colored as in Figure 2.
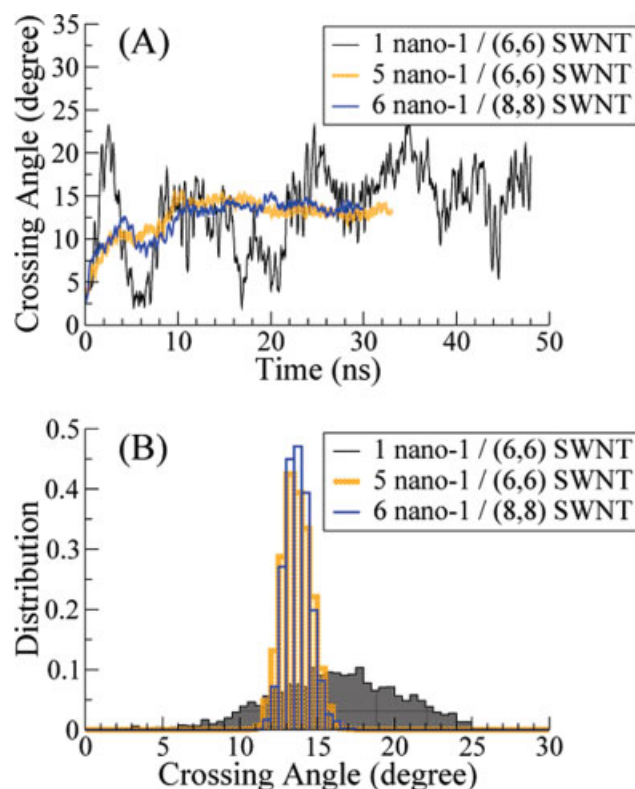
FIGURE 4 (A) Comparison of the crossing angle of a single nano-1/(6,6) SWNT complex (black) from our previous work[26] with the average crossing angle of the pentamer/(6,6) SWNT complex (thick orange), and the hexamer/(8,8) SWNT complex (blue). (B) Crossing angle distributions of the single nano-1/(6,6) SWNT complex from 21 to 48 ns (black), the pentamer/(6,6) SWNT complex from 12 to 33 ns (thick orange), and the hexamer/(8,8) SWNT complex from 12 to 30 ns (blue).

plexes. These distances are about 12.5 ± 0.5 Å for the pentamer/(6,6) SWNT complex. For the hexamer/(8,8) SWNT complex, the axis–axis distances are ~ 12.5 Å ± 1.0 Å, except for the P1-P2 distance which was smaller at about 11 Å due to C-terminal fraying of the P1 peptide. Comparing the two systems, the distances in the pentamer system have less variation across peptide pairs than in the hexamer system, consistent with the α-helicity and crossing angle analysis.

The peptide-SWNT contact area analysis for both multipeptide/SWNT systems are illustrated in Figure 6. The contact ratios for the pentamer/(6,6) SWNT system are $\sim 15\%$, which is consistent with the single peptide/(6,6) SWNT system.[26] In the hexamer/(8,8) SWNT complex, the contact ratios for the peptides are also $\sim 15\%$ except for P1 which has a 17% contact ratio because of the increased contact between His28 and SWNT through the imidazole side chain. The contact area of each peptide in the multipeptide/SWNT complex has as much contact with the SWNT as in the single

peptide system, suggesting that the multipeptide complex does not compromise the ability of each peptide to interact fully with the SWNT.

Figure 7 displays the distribution of the Phe-to-SWNT distance in both multipeptide systems. The distance distributions for both systems are similar, narrow, unimodal, and peaked at 3.5 Å, indicating that all Phe residues adopt parallel π-stacking conformations against the SWNT aromatic surface, consistent with our observations for the single peptide system.[26]

The peptides are observed to interact with each other and form interpeptide H-bonds, which help to stabilize the multipeptide/SWNT complexes. As shown in Figure 8, the total number of H-bonds in the hexamer/(8,8) SWNT complex is very similar to that of the pentamer/(6,6) SWNT complex, despite the increased number of peptides. Moreover, during the 10–20 ns interval, the number of H-bonds in the pentamer system is actually higher than in the hexamer system. However, if we focus on the solvation environment of the two multipeptide systems, we find almost no difference.
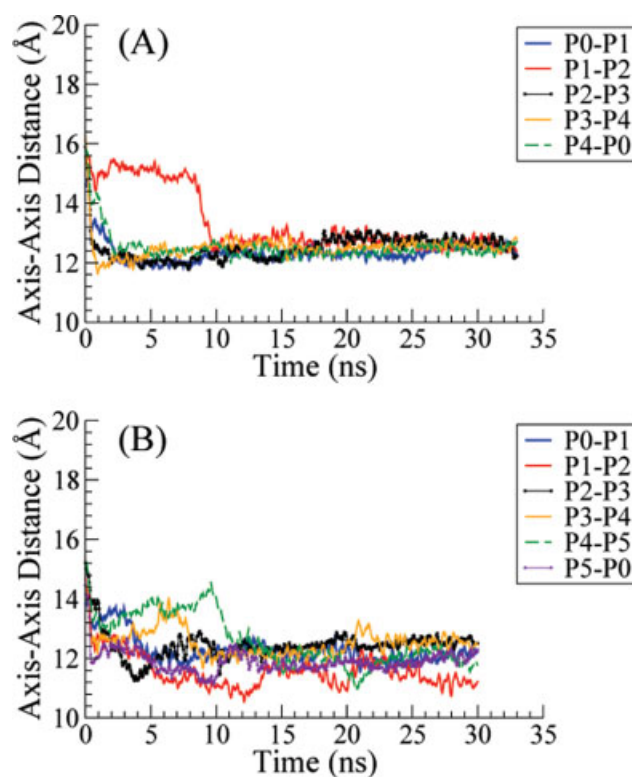

FIGURE 5 The peptide helical axis-to-axis distance for adjacent peptide pairs in the (A) pentamer/(6,6) SWNT and (B) hexamer/(8,8) SWNT systems as a function of time. The peptide pairs are marked as P0-P1 (blue), P1-P2 (red), P2-P3 (black), P3-P4 (orange), P4-P0 for the pentamer system or P4-P5 for the hexamer system (green dash), and P5-P0 (purple) for the hexamer system.
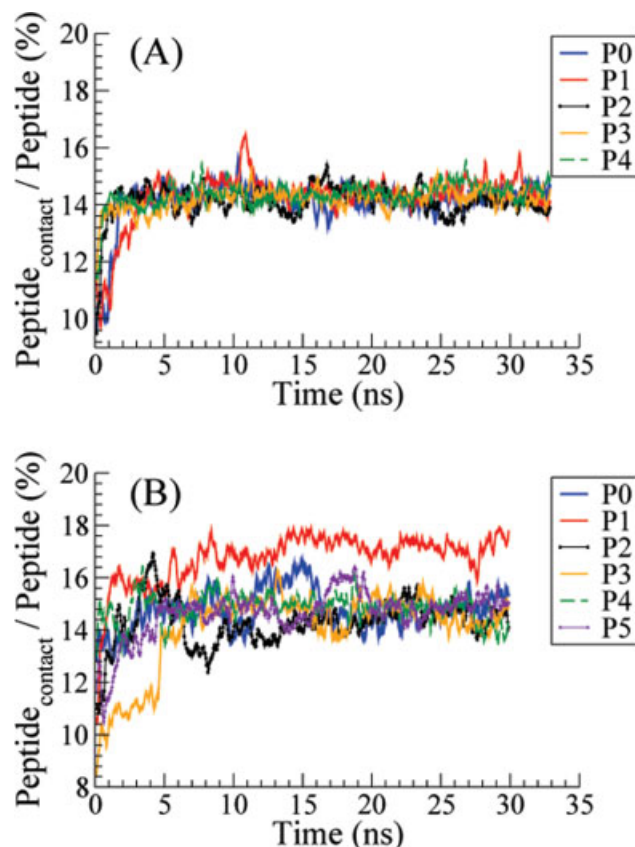
FIGURE 6 The ratio of the contact areas between the peptides and the SWNT surface vs. the total peptide surface area for the (A) pentamer/(6,6) SWNT and (B) hexamer/(8,8) SWNT systems as a function of time. The peptides are colored as in Figure 2.

Namely, comparing the two systems, (1) the SWNT is completely desolvated in the peptide-coated region, (2) the average number of H-bonds per peptide with water is very
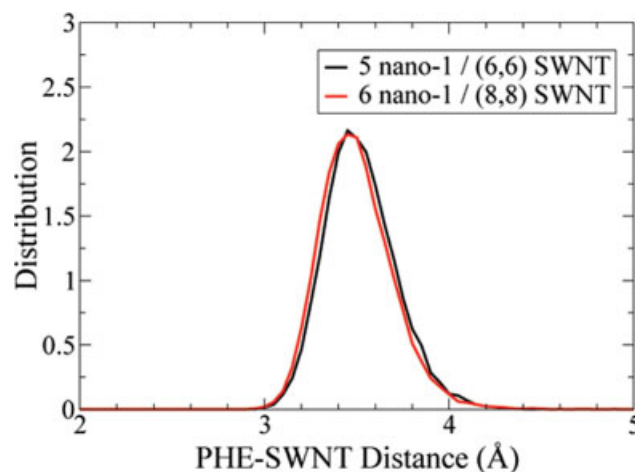

FIGURE 7 The distributions of the distance between the Phe aromatic ring centers and the SWNT surface for the pentamer/(6,6) SWNT complex (black) and the hexamer/(8,8) SWNT complex (red).
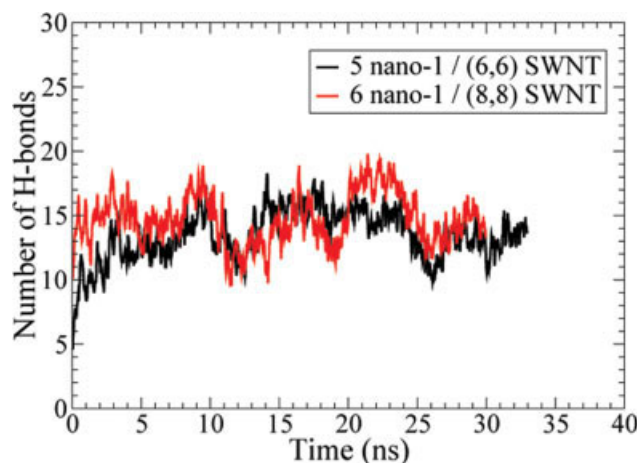

FIGURE 8 The total number of H-bonds formed between the peptide sidechains within the pentamer/(6,6) SWNT complex (black) and the hexamer/(8,8) SWNT complex (red).

similar, and (3) the average number of water molecules between adjacent peptide pairs is very similar (data not shown).

In summary, from the conformational analysis, axis–axis distance data, contact area analysis and H-bond analysis, it is clear that the peptide conformations and the peptide–peptide distances fluctuate more in the hexamer/(8,8) SWNT system than in the pentamer/(6,6) SWNT system. These results strongly suggests that five nano-1 peptides can pack more tightly around a (6,6) SWNT than six nano-1 peptides around an (8,8) SWNT.

CONCLUSIONS

After 30 ns of simulation, both the pentamer/(6,6) SWNT complex and the hexamer/(8,8) SWNT complex have reached equilibrium. The amphiphilic peptides collectively tilt over the first 10 ns of the simulations from an initially parallel alignment to strongly interact with each other and to completely shield the SWNT from contact with water. All peptides remain α-helical and form inter-peptide H-bonds through their Lys and Glu residues, which helps to stabilize the multipeptide/SWNT complex. All hydrophobic residues interact with SWNT and are sequestered from water.

The Phe-to-SWNT distance distribution is narrow, unimodal, and peaked at 3.5 Å, indicating that all Phe adopt parallel π-stacking conformations and have strong interactions with SWNT; this corroborates our previous study[26] which established that the Phe residues play a dominant role in the peptide-SWNT interactions.

The single peptide/(6,6) SWNT system has a crossing angle distribution from 5° to 25°, which is much wider than the narrow angle distribution of 11° to 17° for both the

pentamer/(6,6) SWNT and hexamer/(8,8) SWNT complexes. The most probable angle for the single peptide system is 17° which is different from the most probable angle of 13° for the multipeptide systems. The peptide–peptide interactions limit the peptide's motion on the SWNT, which suppresses the crossing angle thermal fluctuations. The shift in the most probable crossing angle suggests that the interpeptide interactions are significant. But the overall angle distributions of the multi-peptide systems fall inside the distribution range of the single peptide system, showing that the interpeptide interactions do not destabilize the peptide-SWNT interactions. For all the systems studied, the most probable crossing angle is consistent with the crossing angle range of 10° to 20° from experimental data. Note, however, that the systems studied here included solvent molecules, whereas the experimental data is obtained from dehydrated samples.

Combining all of the data analysis, it is clear that the peptide conformations and the peptide–peptide distances fluctuate more in the hexamer/(8,8) SWNT system. This strongly suggests that five nano-1 peptides can pack more tightly around a (6,6) SWNT than six nano-1 peptides on an (8,8) SWNT. The contact area analysis shows that the peptides in the multipeptide/SWNT complexes have as much contact with the SWNT as in the single peptide system, suggesting that the multipeptide complexes do not compromise the ability of each peptide to interact with SWNT. This again supports the notion that nano-1 is an excellent dispersal agent for SWNTs.

REFERENCES

1. Saito, R.; Dresselhaus, G.; Dresselhaus, M. S. Physical Properties of Carbon Nanotubes; Imperial College Press: London, 1998.
2. Baughman, R. H.; Zakhidov, A. A.; de Heer, W. A. Science 2002, 297, 787–792.
3. Tasis, D.; Tagmatarchis, N.; Georgakilas, V.; Prato, M. Chem Eur J 2003, 9, 4000–4008.
4. Banerjee, S.; Hemraj-Benny, T.; Wong, S. S. Adv Mater 2005, 17, 17–29.
5. Lin, Y.; Elkin, T.; Taylor, S.; Gu, L. R.; Chen, B. L.; Veca, L. M.; Zhou, B.; Yang, H.; Brown, J.; Joseph, R.; Jones, E.; Jiang, X. P.; Sun, Y. P. Microchimica Acta 2006, 152, 249–254.
6. Huang, W.; Taylor, S.; Fu, K.; Lin, Y.; Zhang, D.; Hanks, T. W.; Rao, A. M.; Sun, Y.-P. Nano Lett 2002, 2, 311–314.
7. Elkin, T.; Jiang, X.; Taylor, S.; Lin, Y.; Gu, L.; Yang, H.; Brown, J.; Collins, S.; Sun, Y.-P. ChemBiochem 2005, 6, 640–643.
8. O'Connell, M. J.; Boul, P.; Ericson, L. M.; Huffman, C.; Wang, Y.; Haroz, E.; Kuper, C.; Tour, J.; Ausman, K. D.; Smalley, R. E. Chem Phys Lett 2001, 342, 265–271.
9. Mitchell, C. A.; Krishnamoorti, R. Macromolecules 2007, 40, 1538–1545.
10. Vaisman, L.; Wagner, H. D.; Marom, G. Adv Colloid Interface Sci 2006, 128, 37–46.
11. Wallace, E. J.; Sansom, M. S. P. Nano Lett 2007, 7, 1923–1928.
12. Qiao, R.; Ke, P. C. J Am Chem Soc 2006, 128, 13656–13657.
13. Chen, R. J.; Zhang, Y.; Wang, D.; Dai, H. J Am Chem Soc 2001, 123, 3838–3839.
14. Daniel, S.; Rao, T. P.; Rao, K. S.; Rani, S. U.; Naidu, G. R. K.; Lee, H. Y.; Kawai, T. Sens Actuators B-Chem 2007, 122, 672–682.
15. Gao, H. J.; Kong, Y. Ann Rev Mater Res 2004, 34, 123–150.
16. Zheng, M.; Jagota, A.; Semke, E. D.; Diner, B. A.; Mclean, R. S.; Lustig, S. R.; Richardson, R. E.; Tassi, N. G. Nat Mater 2003, 2, 338–342.
17. Noon, W. H.; Kong, Y. F.; Ma, J. P. Proc Natl Acad Sci USA 2002, 99, 6466–6470.
18. Chen, B.-X.; Wilson, S. R.; Das, M.; Coughlin, D. J.; Erlanger, B. F. Proc Natl Acad Sci USA 1998, 95, 10809–10813.
19. Braden, B. C.; Goldbaum, F. A.; Chen, B.-X.; Kirschner, A. N.; Wilson, S. R.; Erlanger, B. F. Proc Natl Acad Sci USA 2000, 97, 12193–12197.
20. Dieckmann, G. R.; Dalton, A. B.; Johnson, P. A.; Razal, J.; Chen, J.; Giordano, G. M.; Munoz, E.; Musselman, I. H.; Baughman, R. H.; Draper, R. K. J Am Chem Soc 2003, 125, 1770–1777.
21. Dalton, A. B.; Ortiz-Acevedo, A.; Zorbas, V.; Brunner, E.; Sampson, W. M.; Collins, S.; Razal, J. M.; Yoshida, M. M.; Baughman, R. H.; Draper, R. K.; Musselman, I. H.; Jose-Yacaman, M.; Dieckmann, G. R. Adv Funct Mater 2004, 14, 1147–1151.
22. Zorbas, V.; Smith, A. L.; Ortiz-Acevedo, A.; Xie, H.; Dalton, A. B.; Dieckmann, G. R.; Draper, R. K.; Baughman, R. H.; Musselman, I. H. J Am Chem Soc 2005, 127, 12323–12328.
23. Zorbas, V.; Ortiz-Acevedo, A.; Dalton, A. B.; Yoshida, M. M.; Dieckmann, G. R.; Draper, R. K.; Baughman, R. H.; Jose-Yacaman, M.; Musselman, I. H. J Am Chem Soc 2004, 126, 7222–7227.
24. Ogihara, N. L.; Weiss, M. S.; DeGrado, W. F.; Eisenberg, D. Prot Sci 1997, 6, 80–88.
25. Nymeyer, H.; Woolf, T. B.; Garcia, A. E. Proteins-Struct Funct Bioinform 2005, 59, 783–790.
26. Chiu, C. C.; Dieckmann, G. R.; Nielsen, S. O. J Phys Chem B 2008, 112, 16326–16333.
27. Xie, H.; Ortiz-Acevedo, A.; Baughman, R. H.; Draper, R. K.; Musselman, I. H.; Dalton, A. B.; Dieckmann, G. R. J Mater Chem 2005, 15, 1734–1741.
28. Phillips, J. C.; Braun, R.; Wang, W.; Gumbart, J.; Tajkhorshid, E.; Villa, E.; Chipot, C.; Skeel, R. D.; Kale, L.; Schulten, K. J Comp Chem 2005, 26, 1781–1802.
29. Alagona, G.; Ghio, C.; Giolitti, A.; Monti, S. Theor Chem Acc 1999, 101, 143–150.
30. Priyakumar, U. D.; MacKerell, A. D. J Chem Theory Comp 2006, 2, 187–200.
31. Banavali, N. K.; MacKerell, A. D. J Mol Biol 2002, 319, 141–160.
32. Ryckaert, J. P.; Ciccotti, G.; Berendsen, H. J. C. J Comp Phys 1977, 23, 327–341.
33. Andersen, H. C. J Comp Phys 1983, 52, 24–34.
34. Jorgensen, W. L.; Chandrasekhar, J.; Madura, J. D.; Impey, R. W.; Klein, M. L. J Chem Phys 1983, 79, 926–935.
35. Lifson, S.; Roig, A. J Chem Phys 1961, 34, 1963–1974.
36. Kahn, P. C. Comput Chem 1989, 13, 185–189.
37. Sanner, M. F.; Olson, A. J.; Spehner, J. C. Biopolymers 1996, 38, 305–320.
38. Luzar, A.; Chandler, D. Phys Rev Lett 1996, 76, 928–931.